ARMA/USRMS 06-1089

Long-term evolution of the transport proprieties of a fracture from the Coso Geothermal Reservoir

Faoro, I., Yasuhara[1], H., Grader[2], A., Halleck[2], P., Elsworth[2], D. and Marone, C

College of Earth and Mineral Sciences, Penn State University, University Park, Pa 16802, USA

[1]Department of Civil Engineering, Ehime University, Matsuyama, Japan

[2]Energy Institute, Penn State University, University Park, Pa 16802, USA

This paper was prepared for presentation at Golden Rocks 2006, The 41st U.S. Symposium on Rock Mechanics (USRMS): "50 Years of Rock Mechanics - Landmarks and Future Challenges.", held in Golden, Colorado, June 17-21, 2006.

ABSTRACT: Results are reported for a long-term circulation test on a calcite-filled fracture in diorite from the Coso Geothermal Field, California. The fracture is circulated by DI water at 20^o, then 60^o, and then 90^{o}C but under a near constant effective stress of 13 MPa. Through the initial stages of the test, at 20^{o}C, the fracture aperture drops from an initial mean hydraulic aperture of 30 µm to 0.6 µm in the first 100 hours, before reaching a steady magnitude. This corresponds to a net reduction of ~4 orders of magnitude through the initial duration of the experiment, and under constant stress. As temperature is incremented, the average aperture further reduces, but a periodic change in aperture and corresponding hydraulic impedance is recorded under conditions of constant stress, temperature and pressure-controlled flow rate. The peak cyclic flow rate climbs rapidly to of the order of 20 times the steady magnitude, with a period of 6000 minutes, and is interpreted as periodic clogging and flushing of mineral mass from the constricted and brecciated end of the sample. As the temperature is augmented to 90°C the hydraulic impedance continues to decrease, ultimately reaching a final aperture of 1 µm and 0.03 cc/min. This low magnitude of ultimate permeability persists, despite visible open voids within the calcite vein, implicating that much of this porosity is not well connected. Since effective stresses remain constant, this observed response is strongly conditioned by the evolving aqueous chemistry of the sample. Analysis of the recovered data continues.

1. INTRODUTION

Paths of stress, temperature, and chemical potential are known to strongly influence the evolution of the transport proprieties of rocks. This is especially true where the materials are fractured, and permeability is strongly coupled to relatively small changes in fracture apertures, that may in turn be driven by changes in stress or chemical potential. Data constraining the role of stress-mediated chemical effects in fractures are sparse, but are available at elevated temperatures (>300^{o}C) in granite [Moore et al., 1994], and at lower temperatures (50^{o}C-150^{o}C) in tuff [Lin et al., 1990]. These are augmented by results for available composite aggregates of quartz [Elias and Hajash, 1992], halite [Gratier, 1993], calcite [Zhang et al., 1994] and albite [Hajash et al., 1998], at moderate temperatures (23^{o}C-150^{o}C), and the same material suites at elevated temperatures and pressure [Siddiqi et al., 1997]. The limited studies on fractures [Moore et al., 1994; Lin et al., 1990; Durham et al., 2001; Polak et al., 2003; Polak et al., 2004; Yasuhara et al., 2004] suggest an increased sensitivity of their transport proprieties to thermal, hydraulic, mechanical, and chemical processes, over porous medium flows. This is apparent even at temperatures as low as 100^{o}C, where the mobile dissolved species in silica, the test duration is of order of a month [Elias and Hajash, 1992; Lin et al., 1997; Polak et al., 2003], and where permeability may be reduced by a factor of 10^4 [Lin et al.,1990; Polak et al., 2003].

Importantly, fracture permeabilities may either reduce or increase, in surprising ways, depending on the paths of stress or chemical potential. We illustrate this behavior through observations during flow–thought tests on a sample of diorite core containing a natural calcite fracture from the Coso Geothermal Field in Coso, California.

2. EXPERIMENTAL ARRANGEMENT

Flow-through experiments are conducted and reported on fractured samples confined within an X-ray transparent cell to evaluate the influence of stress-mediated changes in dissolution and precipitation on the evolution in transport proprieties. Cylindrical samples containing a single fracture are confined within a flexible membrane and end-to-end flow tests completed, as illustrated in Figure 1.

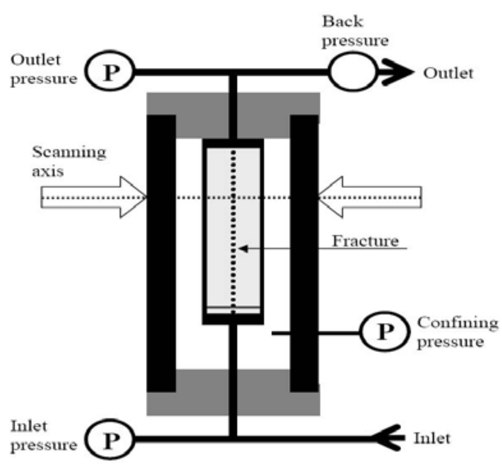

Figure1: Experimental arrangement showing confining cell and sample with axial fracture. Flow at prescribed flow-rate and pressure drop records permeability. Constraint on process is provided by measurement of dissolved mass efflux, and periodic scanning by X-ray CT. [Polak et al., 2003]

Three independent measurements are made to constrain the processes promoting the redistribution of mineral mass within the fracture: hydraulic flux, mineral mass flux, and volumetric imagining by X-ray CT. First, permeability is monitored continuously by prescribing flow rate and measuring pressure drop across the sample. Effective stresses are retained within a narrow range by controlling the upstream pressure. This measurement records permeability, and through this defines change in average aperture within the system. Second, the net efflux of dissolved mineral mass is measured periodically to provide a record of net mass removal, and to correlate this with observed changes in aperture, defined by the flow tests. Finally, periodic non-destructive imaging by X-ray CT is used to view redistribution of mineral mass within the heated sample, as illustrated in figure 2. X-ray CT records changes in density within the sample as a proxy for mineral removal or redistribution, with the scanner used in this study capable of resolving down to ~1/1000th of the diameter of the sample. For the sample diameter of 5 cm used in the following study, the minimum voxel size scales to the order of ~50 μm. This resolution is at the limits of utility in defining mass redistribution, but it is able to confirm that small changes in porosity at important constricted locations exert a disproportionate impact on permeability.

The scanner used is an industrial third-generation microCT machine in the Center for Quantitative imaging at Penn State. The sample was scanned under confining stress through the X-ray transparent vessel. Complete 3-D volume scans were takenat the start and the end of the experiment, with additional partial scans during the experiment. Each full scan consists of X-ray absorption values of a $1024 \times 1024 \times 1150$ of the volume elements (voxels) that make up the sample. A commercial software package was used to extract the fracture volume from the rest of the sample. This is done by setting a threshold that separates the empty voxels of the fracture network from solid-filled voxels of the adjacent rock matrix. A percolation algorithm was then applied to the fracture network to determine connectivity between different portions of the fracture network. Given quantitative compatibility between image sets, the same procedure is applied to data taken before and after the experiment. Comparison of the two fracture networks allows comparison of the changes that have occurred with observed changes hydraulic proprieties.

These measurements provide unusual constraint on the evolving processes. Importantly, they allow the source of dissolved components to be determined: we need to discriminate whether the source is from free-face dissolution of the fracture wall, or from stress-mediated dissolution at contacting asperities. This distinction is crucial since these two mechanisms impart opposite effects in the sense of permeability change, under net dissolution: free-face dissolution increases permeability, and pressure solution reduces permeability

3. EXPERIMENTAL OBSERVATIONS

Experimental observations record the redistribution of mineral mass within the sample through imaging, through the proxy of hydraulic response, and through measurements of the dissolved chemical efflux. The concurrent resolution of these three signals, adds constraint to the dominant processes which control the evolution of the mechanical and chemical response of fractures. Changes in aperture may be followed through imaging, through the reduction of the hydraulic aperture, and through measurement of the mass lost within the sample, also reduced to an equivalent change in aperture. These ensemble signals are described in the following.

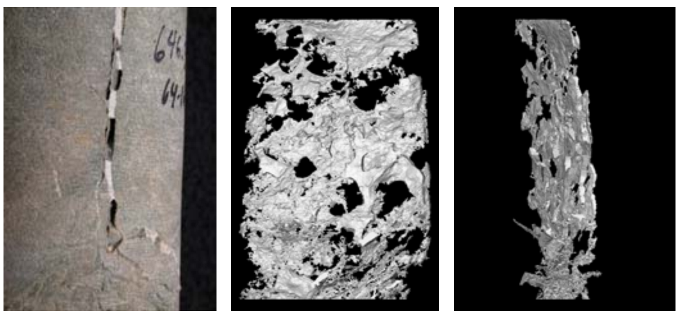

Figure 2. (a) Image of Coso core showing fracture infilled with calcite vein material, and voids. CT Images of the Coso core prior to circulation of fluid. (b) Face-on view, and (c) View of fracture rotated by 90^o.

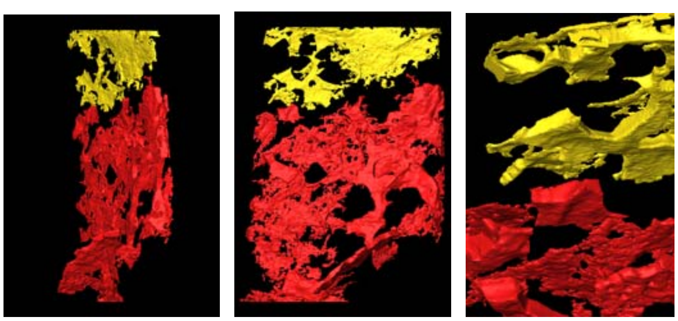

Figure 3. Post-circulation images color-coded for connected porosity. The two colors denote disconnected fracture void volumes: (a) 90^o rotated, (b) Front-on view, (c) Close-up of disconnected portion of the fracture.

3.1. Imaging

The experiment is completed on a core sample of diorite from a depth of 200 m above the Coso Geothermal Field. The sample contains a single through-going vein of calcite with multiple large tabular voids, as illustrated in Figure 2(a). X-ray CT imaging of the core was completed pre- and post-experiment. The imaging shows the main conductive feature of the core – the central calcite vein containing numerous large tabular voids. These large voids occupy about 10% of the fracture volume, as illustrated in Figures 2 (b) and (c), showing both the large voids and the smaller-aperture connected porosity. At the completion of the experiment, re-scanning notes changes in connectivity within the sample. The discrimination of connected porosity is a strong function of the threshold selected for the scanning – and not absolute. However, scanning is able to suggest that the large changes in permeability, witnessed in the hydraulic results, occur as a result of necking-off of the fracture. At a particular CT threshold, the connected porosity divides into two distinct portions, as evident in Figures 3(a) and 3(b). The constricted transport pathway is strongly defined, involving a volume of a few voxels, as illustrated in the close-up of Figure 3(c). Clearly, since the sample is always hydraulically connected, the porosity is connected between the upper and lower parts of the fracture – although it is severely constricted.

3.2. Hydraulic Behavior

The evolution of the fracture aperture is the second signal which may be followed with the progress of the experiment. The equivalent hydraulic aperture, b, is related to the recorded flow rate, Q and the pressure drop, dp, measured over the sample length, dl, as:

$$Q = d \cdot \frac{b^3}{12\mu} \cdot \frac{dp}{dl} \qquad (1)$$

where d is the diameter of the cylindrical sample with a diametral fracture. This allows aperture to be used as a proxy for average change in the transport characteristics, as a common reference between imaging and inferred changes in transport characteristics due to precipitation and dissolution. The progress of aperture change measured from the hydraulic response is shown in Figure 4, for an experiment conducted at a constant effective stress of 13 MPa and at incremented temperatures of 20^o, 60^o, and 90^{o}C.

The response shows a rapid reduction in aperture from 30μm under initial ambient stress and at 20^{o}C to less than 1μm as the flow-through experiment continues, as illustrated in Figure 4(a). After this initial closure in the first 100 hours, which never recovers, the aperture remains roughly constant in average magnitude, except for monotonic peaks and crests in calculated aperture which correlate with spikes in flow rate, for the experiment conducted under controlled pressure drop. These spikes in pressure appear to be in response to the plugging and then clearing of the fracture flow path. The post blockage episodes exhibit elevated mass concentrations, as illustrated in Figure 4(b). This coherence in the signal suggests that fluid is locked behind an obstruction within the reservoir of the fracture void, before the blockage is cleared. This implicates precipitation or obstruction by a mechanical blockage as causing this observed pulse in flow rate. The regular and repeating periodic nature of the blockage and purging signal suggests a characteristic response of the system, and favors control by precipitation, rather than by the random bridging by a trapped particle.

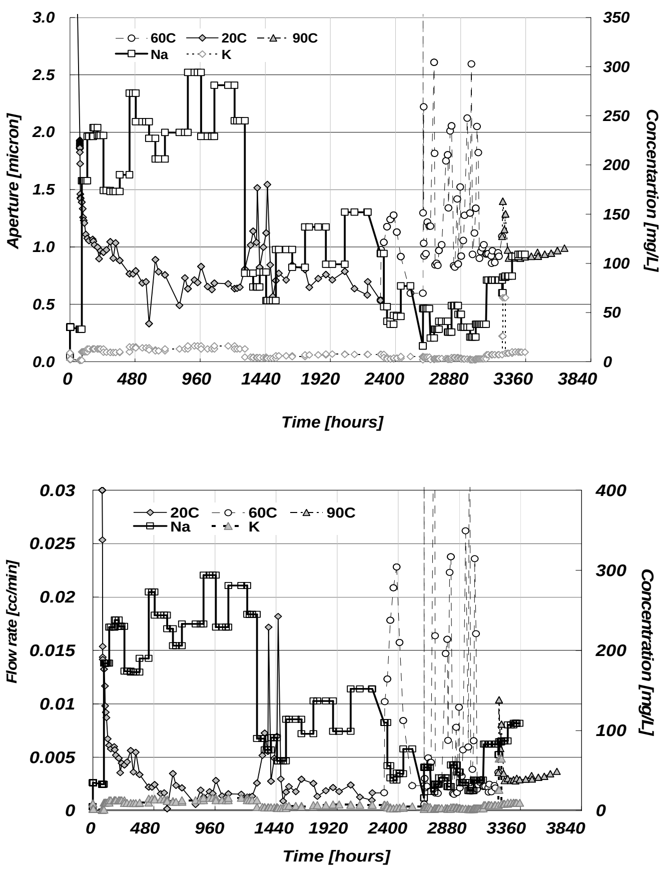

Figure 4: [a] Change in hydraulic aperture with test duration together with mass concentrations of major ions. [b] Change in concentration of major ions with flow rate. Injection at 20°, 60°, and 90°C.

3.3. Chemical Behavior

Continuous measurements of the dissolved mass removed from the sample allow the cumulative mass removed to be evaluated. For a mass M removed in a given time interval, the equivalent change in aperture may be evaluated from the density of the dissolved mineral, ρ and the presumed surface area of removal, A_c, as $\Delta b=MA_c/\rho$. The mass removed is recovered from the product of volumetric flow rate, Q, and mass concentration, c, as $M=Qc$.

Where the system is far from equilibrium, and net dissolution prevails, net reduction in aperture suggests that mineral mass is being removed from the bridging asperities, and where aperture increases, then removal from the exposed free faces prevails. In each case, the active area of interest will be the asperity contact area, or the free face area, respectively.

These characterizations may be used to follow the cumulative mass removed from the fracture with time, as illustrated in Figure 5. The total mass removed from all sources over the 4000 hour-long experiment total *100mg* from all sources. Of this the principal component is sodium accounting for 84% of the total.

Paradoxically, the signal for cumulative mass removed is not consistent with the aperture change. The aperture change occurs very early within the experiment, and is complete within the first 100 hours. However, mass continues to be removed from the fracture, and without any apparent change on the hydraulic response. This is apparent, even as temperatures are augmented with the progress of the experiment.

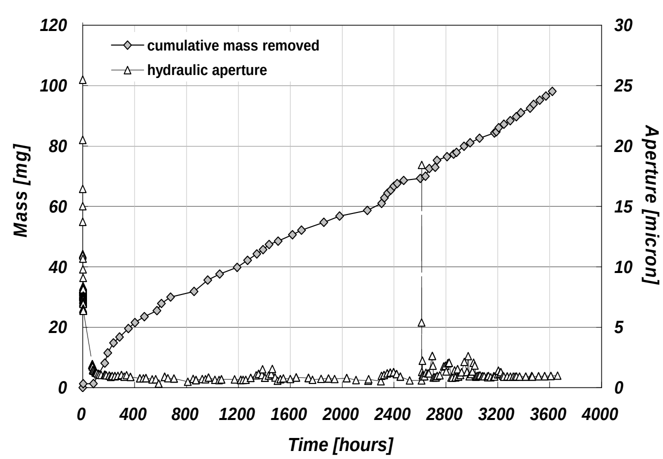

Figure 5. Change in aperture determined from measured change in dissolved mass removed.

3.4. Process-Based Interpretations

Principal observations for this experiment are that despite continuous net dissolution throughout, the transmissive aperture of the fracture decreases. This could infer the removal of material from beneath bridging asperities, under the action of pressure dissolution, as has been implicated elsewhere [Polak et al., 2003; Yaushara et al., 2004]. The rates of mass removal are of the same order as the rate of change in fracture aperture, as illustrated in Figure 6. For removal of mass from a contact area of 20% of the total fracture area, results in a ~30μm change in aperture, close to that recorded throughout the duration of the experiment. However, the timing of this removal is not congruent with the observed change in aperture, as recorded from the hydraulic signal. To reconcile this mismatch in hydraulic and chemical observations, we consider a model of asperity crushing driven by local stresses at the asperity contacts. In this, the locally elevated stresses are able to fracture the calcite layer separating the asperity walls. This results in a rapid reduction in aperture as the material crushes, as illustrated in Figure 7(a). This comminution results in elevated rates of mass dissolution (Figure 7(b)) but with negligible reduction in aperture, due to an underlying asperity structure. This elevation in dissolution rates is reflected in the elevated mass removal rate recorded in the first portion of the experiment at 20°C. At the incrementing of temperature, this dissolution rate is sequentially elevated. This suggests that new fracturing is initiated with the addition of each temperature increment, possibly due to a slight reduction in the critical stress for pressure solution to begin, as illustrated in Figure 8, although this suggests much smaller contact areas than those suggested by the chemical dissolution record.

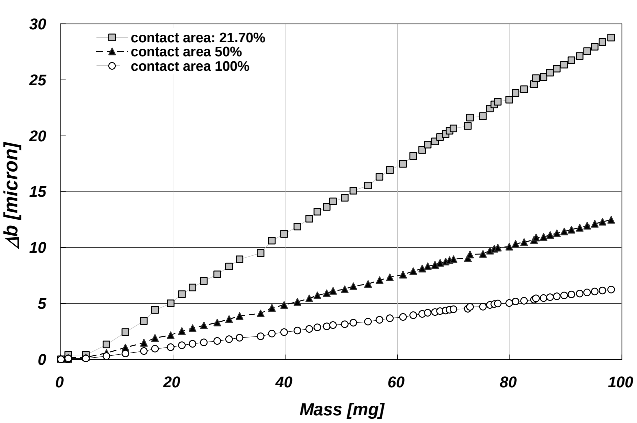

Figure 6. Changes in aperture produced for various contact area ratios of the contacting fracture.

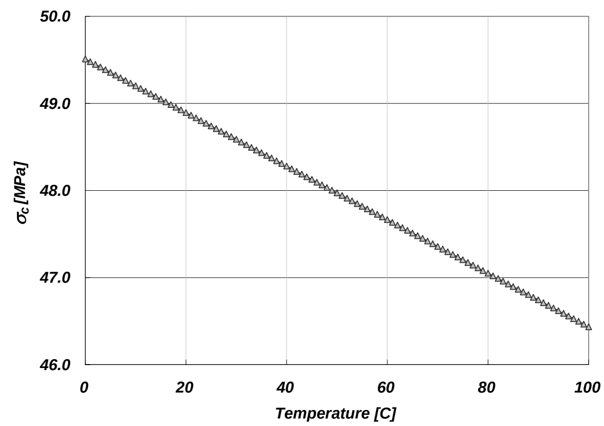

Figure 7. Process model of change in aperture with applied stress.

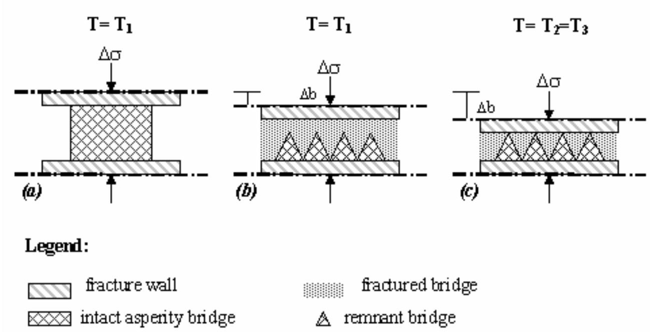

Figure 8. Change in critical stress with temperature for the experimental temperature of 20°, 60°, and 90°C.

4. DISCUSSION AND CONCLUSIONS

Preliminary results are shown for changes in permeability which result from the circulation of reactive fluid within a fracture. The change in aperture is severe, resulting in a decrease from 30μm to 1μm in the first 100 hours of the experiment, corresponding to a reduction in permeability of over four orders of magnitude.

Although the measured change in equivalent aperture, recovered from the hydraulic measurements, is of the same order as the cumulative mineral mass removed, the events are not coherent. The hydraulic change occurs rapidly, although the removal of mineral mass continues near continuously throughout the experiment. A preliminary model is suggested which honors these observations. This comprises the crushing of contacting asperity contacts, leaving crushed vein material with increased surface area for dissolution. This gives an elevated dissolution signature immediately post-crushing, which then drops with time. This behavior is observed in the response.

Although preliminary, these observations note the important influence of chemistry on the mechanical and transport properties of rocks, and in particular the sensitivity of fractures to these effects.

Acknowledgements: This work is the result of partial support from the US Department of Energy under project DOE-DE-FG36-04GO14289. This support is gratefully acknowledged. We thank Peter Rose for supplying the core sample from the EGI Core Bank.

REFERENCES

1. Moore, D. E., D. A. Lockner, et al. (1994). "Reduction of Permeability in Granite at Elevated-Temperatures." Science 265(5178): 1558-1561.
2. Lin, W. N. and W. Daily (1990). "Hydrological Properties of Topopah Spring Tuff under a Thermal-Gradient - Laboratory Results." International Journal of Rock Mechanics and Mining Sciences & Geomechanics Abstracts 27(5): 373-&.
3. Elias, B. P. and A. Hajash (1992). "Changes in Quartz Solubility and Porosity Due to Effective Stress - an Experimental Investigation of Pressure Solution." Geology 20(5): 451-454
4. Zhang, S. Q., S. F. Cox, et al. (1994). "The Influence of Room-Temperature Deformation on Porosity and Permeability in Calcite Aggregates." Journal of Geophysical Research-Solid Earth 99(B8): 15761-15775
5. Hajash, A., T. D. Carpenter, et al. (1998). "Dissolution and time-dependent compaction of albite sand: experiments at 100 degrees C and 160 degrees C in pH-buffered organic acids and distilled water." Tectonophysics 295(1-2): 93-115.
6. Siddiqi, G., B. Evans, et al. (1997). "Effect of semibrittle deformation on transport properties of calcite rocks." Journal of Geophysical Research-Solid Earth 102(B7): 14765-14778.
7. Durham, W. B., W. L. Bourcier, et al. (2001). "Direct observation of reactive flow in a single fracture." Water Resources Research 37(1): 1-12
8. Polak, A., D. Elsworth, et al. (2004). "Spontaneous switching of permeability changes in a limestone fracture with net dissolution." Water Resources Research 40(3): -.
9. Yasuhara, H., D. Elsworth, et al. (2004). "Evolution of permeability in a natural fracture: Significant role of pressure solution." Journal of Geophysical Research-Solid Earth 109(B3): -.
10. Polak, A., D. Elsworth, et al. (2003). "Permeability reduction of a natural fracture under net dissolution by hydrothermal fluids." Geophysical Research Letters 30(20): -.
11. Gratier, J. P. (1993). "Experimental Pressure Solution of Halite by an Indenter Technique." Geophysical Research Letters 20(15): 1647-1650.